Proceedings of the 20th Jerusalem Symposium, May 1987

CONF-8705209--1

CONF-8705209--1

DE88 000397

ELECTRON LOCALIZATION IN WATER CLUSTERS

Uzi Landman, R.N. Barnett and C.L. Cleveland
School of Physics, Georgia Institute of Technology
Atlanta, Georgia 30332, U.S.A. and
Joshua Jortner, School of Chemistry
Tel-Aviv University, 69978 Tel-Aviv, Israel

ABSTRACT

Electron attachment to water clusters was explored by the quantum path integral molecular dynamics method, demonstrating that the energetically favored localization mode involves a surface state of the excess electron, rather than the precursor of the hydrated electron. The cluster size dependence, the energetics and the charge distribution of these novel electron-cluster surface states are explored.

I. INTRODUCTION

Isolated clusters provide ways and means for the exploration of the evolution of size effects on energetic, dynamic and chemical phenomena in large, finite systems[1]. Studies of the structure, the level structure and the dynamics of clusters do not solely manifest the "transition" from molecular to condensed matter systems, but also provide a bridge between molecular and surface phenomena, as is evident from experimental studies of microscopic catalysis on metal clusters[2] and from theoretical investigations of surface states for an excess electron on alkali halide clusters[3]. The formation of a cluster-electron surface state is facilitated by the large surface to volume ratio of the cluster, being determined by the cluster structure, its degree of aggregation and the nature of the electron-cluster interactions. We shall demonstrate, using quantum path integral molecular dynamics simulations[3,4] (QUPID), that the energetically stable excess electron states in small water clusters[5-7] involve surface states rather than internally localized states which may be regarded as precursors of the celebrated hydrated electron.[8]

The existence of the solvated electron was experimentally demonstrated in 1863 for liquid ammonia[9] and in 1962 for water.[8] The localization of an excess electron in the bulk of a polar fluid originates from the combination of long-range and short-range attractive interactions,[10] and is accompanied by a large local molecular reorganization. Nonreactive electron localization in water clusters was

FG05-86ER45234

experimentally documented to originate either from electron binding during the cluster nucleation process,[5,6] or by electron attachment to preexisting clusters.[7] The occurrence of a weakly bound state in $(H_2O)_2^-$ (vertical electron binding energy -3 meV for the equilibrium state[11,12] and -13 to -27 meV for a persistent metastable state),[12] characterized by a diffuse excess electron charge distribution (radius of gyration of $\sim 36a_0$)[11,12] can be understood on the basis of QUPID calculations, to originate from weak electron-dipole interactions. On the other hand, the experimental observation of stable $(H_2O)_n^-$ ($n > 11$) clusters,[5-7] which are characterized[7] by a large vertical electron binding energy, i.e., -0.7 eV (for $n = 11$) to -1.2 eV (for $n = 20$), poses a challenging theoretical problem. Quantum mechanical calculations[13,14] for $(H_2O)_6^-$ and $(H_2O)_8^-$ reveal that the adiabatic electron binding energy of these, and presumably also larger, water clusters will be positive, precluding the existence of such stable excess electron clusters, in contrast with experiment.[5-7] These theoretical studies followed faithfully the conventional wisdom in the field of solvated electron theory,[10] invoking the implicit assumption that the excess electron state in $(H_2O)_n^-$ constitutes an interior localization mode. QUPID calculations are ideally suited to explore alternative localization modes of the excess electron in water clusters.

II ENERGETICS AND INTERACTIONS

The QUPID method rests on an isomorphism between the quantum problem and a classical one, wherein the quantum particle is represented by a necklace of P pseudo-particles ("beads") with nearest-neighbor harmonic interactions.[3,4] Invoking previous formalism and notation[3] the average total energy of the system is $E = 3N/2\beta + \langle V_c \rangle + K + P^{-1}\langle \sum_{i=1}^{P} V(\vec{r}_i) \rangle$ with $K = 3/2\beta + K_{int}$, where V_c is the interaction potential between the classical particles (whose number is N), $V(r_i)$ is the cluster-electron interaction for the ith pseudoparticle, $K_{int} = (1/2P) \sum_{i=1}^{P} \langle (\partial V(\vec{r}_i)/\partial \vec{r}_i) \cdot (\vec{r}_i - \vec{r}_p) \rangle$, $\beta = 1/kT$ and $\langle\ \rangle$ indicates statistical averaging. The water molecules in this study were treated classically. The choise of the number, P, of beads representing the excess electron is temperature dependent. As a rule of thumb, adequate discretization is achieved for $PkT \geq e^2/a_0$.

A key issue in modeling the system is the choice of interaction potentials. Fortunately, for neutral small water clusters, interaction potential functions which provide a satisfactory description for a range of properties are available. We have used the RWK2-M model[15] for the intra and inter-molecular interactions. For the electron water interaction we have constructed a pseudo-potential (Fig. 1) in the spirit of the density functional theory, which consists of Coulomb, polarization, exclusion, and exchange contributions:

$$V(\vec{r}_e,\vec{R}_0,\vec{R}_1,\vec{R}_2) = V_{coul} + V_p + V_e + V_x \quad . \tag{1}$$

The position of the oxygen and hydrogen nuclei of the water molecule are given by $(\vec{R}_0,\vec{R}_1,\vec{R}_2)$ and $\vec{r}_e$ is the position of the electron. The Coulomb interaction is

$$V_{coul}(\vec{r}_e,\vec{R}_0,\vec{R}_1,\vec{R}_2) = -\sum_{j=1}^{3} q_j e/\max(|\vec{r}_e - \vec{R}_j|, R_{cc}) \quad , \tag{2}$$

where $\vec{R}_3 = \vec{R}_0 + (\vec{R}_1+\vec{R}_2-2\vec{R}_0)\delta$ is the position of the negative point charge of the RWK2-M model and $R_{cc} = 0.5a_o$. The values $q_1 = q_2 = 0.6e$, $q_3 = -1.2e$, $\delta = 0.22183756\ a_0$ were chosen[15] to give a good representation of the dipole and quadrupole moments of H_2O. The polarization interaction is given by

$$V_p(\vec{r},\vec{R}_0) = -0.5\alpha e^2/(|\vec{r}_e-\vec{R}_0|^2 + R_p^2)^2 \quad , \tag{3}$$

where $\alpha = 9.7446$ a.u. is the spherical polarizability of the water molecule. The form of V_p and the value of $R_p = 1.6a_0$ were chosen to fit the adiabatic polarization potential as calculated by Douglass et al.[16] The exclusion, V_e, and exchange, V_x, contributions both require the electron density $\rho(\vec{r},\vec{R}_0,\vec{R}_1,\vec{R}_2)$, of the water molecule[17] which, in the regions of importance, is adequately approximated by the simple expression (see Fig. 1)

$$\rho(\vec{r};\vec{R}_0,\vec{R}_1,\vec{R}_2) = 8\,a_o^{-3}\, e^{-3|\vec{r}-\vec{R}_0|/a_0} + a_o^{-3} \sum_{j=1}^{2} e^{-3|\vec{r}-\vec{R}_j|/a_o} . \tag{4}$$

The repulsion, due to the exclusion principle, is modeled as a "local kinetic energy" term,

$$V_e(\vec{r}_e,\vec{R}_0,\vec{R}_1,\vec{R}_2) = 0.5\ e^2 a_0\ (3\pi^2\rho)^{2/3} \quad . \tag{5}$$

The exchange interaction is modeled via the local exchange approximation,

$$V_x(\vec{r}_e,\vec{R}_0,\vec{R}_1,\vec{R}_2) = -\alpha_x e^2 a_0 (3\pi^2\rho)^{1/3}/\pi \tag{6}$$

The parameter α_x was taken to be $\alpha_x = 0.3$ in order to obtain good agreement between our simulation results and the SCF results of Rao and Kestner[13] for $(H_2O)_8^-$ at a fixed configuration of the water molecules.

III SURFACE STATES OF EXCESS ELECTRON ON WATER CLUSTERS

Equipped with these potentials we have embarked upon an investigation of the energetics and geometry of $(H_2O)_n^-$ (n = 8-18) clusters. In correspondence with the alternative experimental preparation methods[5-7] we invoked two initial conditions. (i) First condensing the water molecules around a classical negatively charged particle with a radius of $5a_0$, and subsequently replacing the classical particle with the electron necklace. (ii) Placing a compact distribution of beads next to an

equilibrated neutral cluster. For the smaller clusters $n \lesssim 12$ a surface state develops rapidly, regardless of the initial setup of the calculation, while for $n = 18$ (i) and (ii) yield an "internal" and "surface" state, respectively.

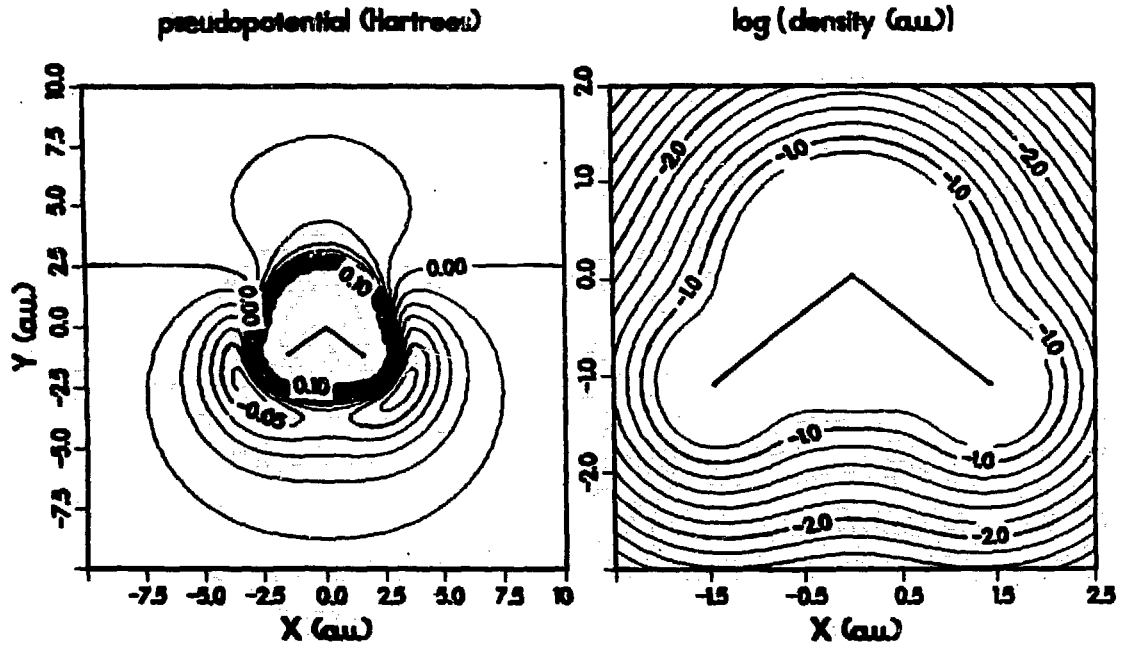

Figure 1: Contours of electron-water interaction, left, and the electron density ($\mathrm{Log}_{10}\rho(r)$), right, (see Eq. 4) in the plane containing the nuclei. The oxygen is located at the origin.

In table I we summarize the energetic data for the electron vertical binding energy, $EVBE = PE(e^-(H_2O)_n) + K_{int}$ where PE is the averaged interaction potential energy between the electron and the water molecules, the cluster reorganization energy, E_c, and the electron adiabatic binding energy, $EABE = EVBE + E_c$. The neutral cluster reference states were obtained by simulated annealing. The lowest energy configuration for each cluster size was then used to calculate E_c (the difference between the molecular potential energies of the negatively charged and neutral clusters). The energetic stability of the negatively charged cluster with respect to the equilibrium neutral cluster plus free electron is inferred from the magnitude and sign EABE, (negative values corresponding to a stable bound state). The bead distributions for the excess electron (Fig. 2) are characterized by the radius of gyration, $R_g^2 = \frac{1}{2P^2} \langle \sum_{i,j} (\underline{r}_i - \underline{r}_j)^2 \rangle$, and the degree of localization by the complex

time correlation function[19] $R(t-t') = \langle|\underline{r}(t)-\underline{r}(t')|^2\rangle^{1/2}$ for $(t-t')\varepsilon(0,\beta h)$, yielding the correlation length $R(\beta h/2)$, (Table 1), which for a free particle is denoted by $R_f = \sqrt{3}\lambda_T/2$, where λ_T is the thermal wavelength of the particle. All calculations were at constant temperature with the velocity form of the Verlet integration algorithm.[20,21]

From these results we assert that there is a remarkable quantitative difference between internal and surface states of the excess electron in water clusters. The value of E_c is considerably lower for a surface state than for an internal state insuring relative energetic stability of the former (Table I). As is apparent for $(H_2O)_{18}^-$, |EVBE| is consierably higher (and outside the range of the experimental values) for the interior state, however, the high value of E_c results in EABE = 0.245 eV, precluding a stable internally localized state. On the other hand, for the electron surface state of $(H_2O)_{18}^-$ the value of EABE is close to zero (and the value of EVBE is in the range of measured values) favoring this mode of localization. For $(H_2O)_{12}^-$ (Table I and Fig. 2), only a surface state is found. Finally, for $(H_2O)_8^-$, a very small electron binding energy is found and the state is characterized by a diffuse charge distribution (Fig. 2 and Table I).

From these results we conclude that: (1) The electron localization mode in $(H_2O)_n^-$ clusters involves the formation of a surface state. (2) The onset of electron localization in a tightly bound state in $(H_2O)_n^-$ clusters is exhibited for $n > 8$, in accord with experiment[5-7] ($n > 11$). (3) The vertical electron binding energy for the cluster-electron-surface-state in $(H_2O)_{12}^-$ and $(H_2O)_{18}^-$ (Table I) are in adequate agreement with the experimental photo-electron spectroscopic data.[7] Additionally, |EVBE| rises sharply in the range $n = 8-12$. For the $(H_2O)_8^-$ cluster the diffuse nature of the excess electron distribution could lead to a large collision induced electron detachment cross-section, which may account for the absence of $n < 11$ clusters from the experimental spectra.[5-7] Considering the complexity of the system, statistical uncertainties and those implicit in the model interaction potentials, we are encouraged by our results which provide a consistent energetic and structural picture of electron localization in small water clusters.

IV CONCLUSIONS

We have demonstrated the prevalence of the surface localization mode in $(H_2O)_n^-$ clusters, which is qualitatively different from the localization mode of the hydrated electron in the bulk. Consequently, we infer that long-range attractive interactions play an important role in electron localization in the bulk. In this context we conjecture that the striking difference[5] between the lowest coordination number for electron localization in water ($n \gtrsim 11$) and that in ammonia ($n \gtrsim 35$) clusters, may originate from a weaker electron-molecule interaction in ammonia, which renders the surface state unstable in $(NH_3)_n^-$ for small n. Consequently localization may require in this case the buildup of long-range attractive interactions thus resulting in large coordination numbers.

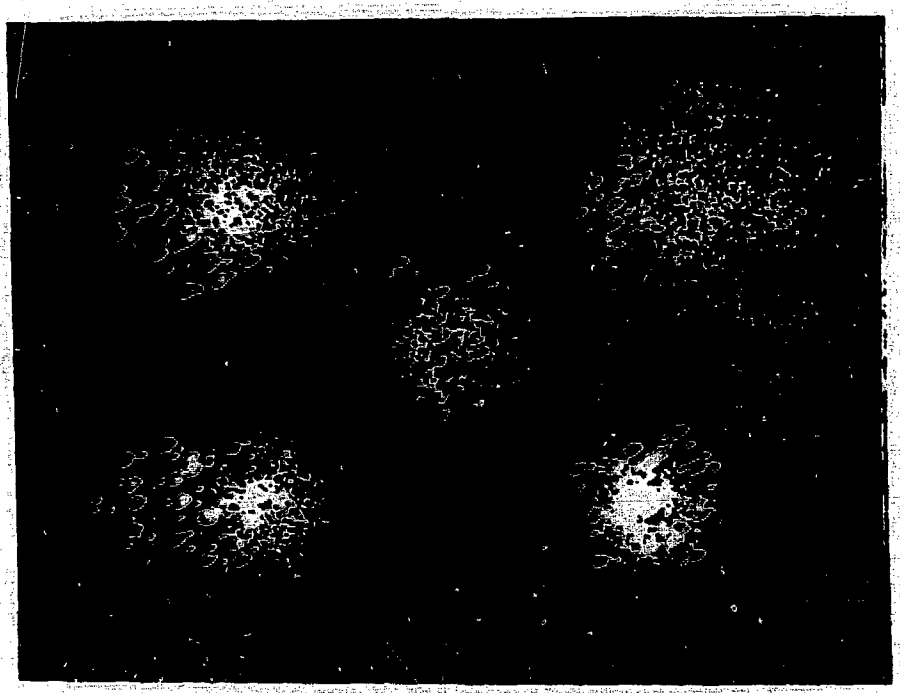

Figure 2: Cluster configurations of $(H_2O)_n^-$, via quantum path-integral molecular dynamics simulations. Balls, large and small, correspond to oxygen and hydrogen, respectively. The dots represent the electron (bead) distributions. Shown at the center is $(H_2O)_8^-$, for a static molecular configuration as in Ref. 13. From top right and going counterclockwise: (i) diffuse surface state of $(H_2O)_8^-$; (ii) surface state of $(H_2O)_{12}^-$; (iii) surface state of $(H_2O)_{18}^-$ and (iv) internal state of $(H_2O)_{18}^-$.

ACKNOWLEDGEMENTS

This research was supported by U.S. DOE Grant No. FG05-86ER45234 (to U.L.) and by the U.S.-Israel Binational Science Foundation (to J.J. and U.L.).

Table I. Energetics and excess electron charge distribution for $(H_2O)_n^-$ clusters. All calculations were at T = 79°K, using P = 4096 beads for the electron necklace. Energies in eV, radius of gyration, R_g, of the electron charge distribution in a_0 units.

CLUSTER	$(H_2O)_8^-$ Diffuse	$(H_2O)_{12}^-$ Surface	$(H_2O)_{18}^-$ Surface	$(H_2O)_{18}^-$ Internal
EVBE	-0.190	-0.97	-1.31	-1.96
E_c	0.136	0.871	1.333	2.204
EABE	-0.054	-0.136	0.023	0.245
R_g	10.6	6.1	5.5	4.1
$\frac{R(\beta\hbar/2)}{R_f}$	0.28	0.15	0.14	0.11

REFERENCES

1. Ber. Bunsenges. Physik. Chem. 88 (1984); Surface Sci. 156, 1-1072 (1985).
2. R.L. Whetten, D.M. Cox, D.J. Trevor, A. Kaldor, Phys. Rev. Lett. 65, 1494 (1985); M.E. Geusic, M.D. Morse, R.D. Smalley, J. Chem. Phys. 82, 590 (1985).
3. U. Landman, D. Scharf and J. Jortner, Phys. Rev. Lett. 54, 1860 (1985).
4. D. Chandler and P.G. Wolynes, J. Chem. Phys. 79, 4078 (1981); M. Parrinello and A. Rahman, ibid. 80, 860 (1985).
5. H. Haberland, H.G. Schindler and D.R. Worsnop, Ber. Bunsenges. Chem. 88, 3903 (1984); J. Chem. Phys. 81, 3742 (1984).
6. J.V. Coe, D.R. Worsnop and K.H. Bowen (J. Chem. Phys., 1987).
7. M. Knapp, O. Echt, D. Kreisle and E. Recknagel, J. Chem. Phys. 85, 636 (1986); J. Phys. Chem. (preprint, 1986).
8. E.J. Hart and J.W. Boag, J. Am. Chem. Soc. 84, 4090 (1962).
9. W. Weyl, Ann. Phys. 197, 601 (1863).
10. J. Jortner, J. Chem. Phys. 30, 839 (1959); D.A. Copeland, N.R. Kestner and J. Jortner, J. Chem. Phys. 53, 1189 (1970).
11. A. Wallquist, D. Thirumalai and B.J. Berne, J. Chem. Phys. 85, 1583 (1986).
12. U. Landman, R.N. Barnett, C.L. Cleveland, D. Scharf and J. Jortner, J. Phys. Chem. (1987), in print.
13. B.K. Rao and N.R. Kestner, J. Chem. Phys. 80, 1587 (1984) and references therein.
14. N.R. Kestner and J. Jortner, J. Phys. Chem. 88, 3818 (1984); M.D. Newton, J. Chem. Phys. 58, 5833 (1973).
15. J.R. Reimers, R.O. Watts and M.L. Klein, Chem. Phys. 64, 95 (1982); J.R. Reimers and R.D. Watts, ibid. 85, 83 (1984). This paper as well as the description of the potential in the first one (Eq. 13 and Table 1) contain several ambiguities and typographical errors. When corrected we reproduce their results.
16. C.H. Douglass, Jr., D.A. Weil, P.A. Charlier, R.A. Eades, D.G. Truhlar and D.A. Dixon, Chemical Applications of Atomic and

Molecular Electrostatic Potentials, Eds., P. Politzer and D.G. Truhlar, (Plenum, New York, 1981), p. 173.
17. C.W. Kerr and M. Karplus in Water, F. Franks, ed., (Plenum, New York, 1972), p. 21; M.W. Ribarsky, W.D. Luedtke and U. Landman, Phys. Rev. B32, 1430 (1985).
18. J.N. Bardsley, Case Studies in Atomic Physics 4, 299 (1974); G.G. Kleiman and U. Landman, Phys. Rev. B8, 5484 (1973).
19. A.L. Nichols, D. Chandler, V. Singh and D.M. Richardson, J. Chem. Phys. 81, 5109 (1984).
20. J.R. Fox and H.C. Anderson, J. Phys. Chem. 88, 4019 (1984).
21. In the QUPID method the averaged results do not depend on the dynamic masses used to generate the classical trajectories. We used a mass of 1 amu for the classical particles and 0.025 amu for the beads. The integration time step was 2.625×10^{-16} sec. Prior to averaging the systems evolved till no discernable trend was observed. Averaging was then performed typically over 2×10^4 time steps.